

Nanofabrication of 1-D Photonic Bandgap Structures Along a Photonic Wire

J. P. Zhang, *Member, IEEE*, D. Y. Chu, S. L. Wu, W. G. Bi, R. C. Tiberio, R. M. Joseph, A. Taflove, *Member, IEEE*, C. W. Tu, *Member, IEEE*, and S. T. Ho, *Member, IEEE*

Abstract—A strongly-guided one-dimensional (1-D) waveguide called a photonic wire has high spontaneous emission coupling efficiency, enabling one to realize low-threshold lasers. Combined with the use of 1-D photonic bandgap structures consisting of arrays of holes etched within the photonic wire, novel microcavity lasers can be realized. We report the nanofabrication of a photonic bandgap structure for 1.5 μm wavelength along a InGaAsP photonic wire, and discuss numerical simulations for its electro-dynamics.

I. INTRODUCTION

THERE has been much interest in the modification of spontaneous emission in artificial photonic structures, including photonic bandgap structures, microcavities, and low-dimensional photonic structures. Recently, low-dimensional photonic structures such as microdisks [1] and photonic wires [2] have been used to realize novel lasers with dimensions and characteristics much different than lasers with conventional structures. For example, the spontaneous emission coupling efficiency β of these lasers, defined as the fraction of spontaneous emission channeled into the lasing mode, can be larger than 10% [3]. In comparison, conventional semiconductor laser structures have $\beta = 0.001\%$. Since spontaneous emission rate and stimulated emission rate are related, a high β value means high gain. It was shown that a high- β value enables

one to achieve low-lasing thresholds and high-modulation bandwidths.

A photonic wire structure is a strongly-guided one-dimensional (1-D) waveguide having tightly-confined modes. Such a waveguide can be formed by a high-refractive-index semiconductor core ($n = 3.4$) surrounded by low-refractive-index cladding such as air ($n = 1$) or SiO_2 ($n = 1.5$). In [3], it was shown that in a strongly-guided waveguide, the photonic density of states can be modified, leading to a significant modification of spontaneous emission in the waveguide. In particular, a large percentage of spontaneous emission can be channeled into the lowest-order guided mode. Recently, a ring microcavity laser based on this concept was demonstrated [2]. This photonic wire laser has a cavity mode volume as small as $0.27 \mu\text{m}^3$ and a spontaneous emission coupling efficiency as high as 35%.

Concurrently, there has been much interest in three-dimensional (3-D) periodic dielectric structures called photonic bandgap structures or photonic crystals [4]. It was shown that by having air voids placed periodically in a high-refractive index material, it is possible to create a bandgap (forbidden frequency band) for the propagation of the electromagnetic field in all directions. Using a similar concept, one expects that a 1-D array of air holes placed in a dielectric waveguide could realize a broad-band Bragg reflector. We refer to such a hole structure as a 1-D photonic bandgap reflector.

Recently, Ho *et al.* and Meade *et al.* suggested that 1-D photonic bandgap reflectors could be fabricated along a photonic wire to form a novel microcavity laser structure [5]–[7]. This structure can be seen as a linear cavity version of the photonic wire ring laser and should also have a high- β value.

In this letter, we report our nanofabrication of the proposed 1-D photonic bandgap structure for operation at the infrared wavelength of 1.5 μm . As shown in Fig. 1, the structure is a tiny photonic wire suspended in air and perforated with holes. It was fabricated on epitaxial layers of InGaAsP that have active quantum-well structures emitting at a wavelength in the 1.5 μm region.

II. 1-D PHOTONIC BANDGAP REFLECTOR

The 1-D photonic bandgap reflector differs from the Bragg reflectors used in vertical cavity surface-emitting lasers and distributed-feedback lasers mainly in its geometry. It consists

Manuscript received October 4, 1995; revised December 11, 1995. The work at Northwestern University was supported by Advanced Research Project Agency contract F30602-94-1-0003, NSF Faculty Early Career Development Award ECS-9502475, and NSF grant ECS-9218494. Work at UCSD was supported by NSF Grant DMR-9202692. The work was performed in part at the Cornell Nanofabrication Facility supported by NSF under Grant ECS-9319005 and Cornell University, and in part at the Northwestern University Material Research Center supported by NSF Grant DMR-9120521.

J. P. Zhang, S. L. Wu, A. Taflove, and S. T. Ho are with the Department of Electrical Engineering and Computer Science, McCormick School of Engineering, Northwestern University, 2145 Sheridan Road, Evanston, IL 60208 USA.

W. G. Bi and C. W. Tu are with the Department of Electrical and Computer Engineering, University of California at San Diego, La Jolla, CA 92093-0407 USA.

R. C. Tiberio is with the National Nanofabrication Facility, Cornell University, Ithaca, NY 14853-5403 USA.

D. Y. Chu was with the Department of Electric Engineering and Computer Science, McCormick School of Engineering, Northwestern University, 2145 Sheridan Road, Evanston, IL 60208 USA. He is now with SDL Inc., 80 Rose Orchard Way, San Jose, CA 95134 USA.

R. M. Joseph was with the Department of Electric Engineering and Computer Science, McCormick School of Engineering, Northwestern University, 2145 Sheridan Road, Evanston, IL 60208 USA. He is now with the Xerox Corporation, 800 Phillips Road, Webster, NY 14580 USA.

Publisher Item Identifier S 1041-1135(96)02607-9.

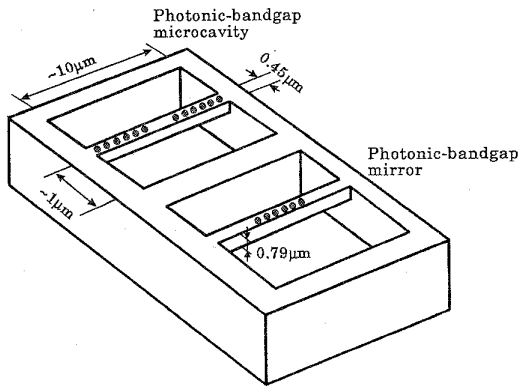


Fig. 1. Schematic diagram of the suspended photonic wire mirror and the corresponding microcavity. The holes were etched in the photonic wire to form a 1-D photonic bandgap structure.

of an array of holes etched into a high refractive index dielectric. An example is shown in Fig. 1 that depicts six holes etched periodically in a photonic wire, and a microcavity formed by two arrays of six holes at each end of the photonic wire.

The guided mode in the photonic wire experiences multiple scattering by the periodic holes, which opens up a frequency bandgap for the propagation of the mode. The center frequency and width of the forbidden band are determined by the size and shape of the holes, the refractive index contrast between the holes and the waveguide, and the spacing between adjacent holes.

We have developed two-dimensional finite-difference time-domain (FD-TD) numerical models for such photonic bandgap structures [8]. The reflection spectrum of the structure is obtained by launching (computationally) a short femtosecond pulse at one end of the waveguide toward the cavity region, and then analyzing the spectrum of the reflected pulse by discrete Fourier transform. The photonic bandgap reflector we considered in the model assumed a 0.3- μm -wide photonic wire with six rectangular holes. The computation was done by choosing a mesh with a uniform spatial resolution of 0.0125 μm . The holes are $0.25 \times 0.1 \mu\text{m}^2$, and the spacing between them is 0.225 μm . This initial 2-D model assumes no spatial variation in the direction perpendicular to the simulation plane. That is, the height of the holes is assumed to be unbounded.

Fig. 2 graphs (dashed line) the computed reflectivity of the six-hole photonic bandgap structure as a function of wavelength. We see that this photonic bandgap structure is a broad-band reflector with about 450-nm bandwidth, and reflectivity as high as 0.98.

We found that the Bragg center wavelength λ_B is given approximately by $\lambda_B/2 = n_{1\text{eff}}d_1 + n_{2\text{eff}}d_2$, where d_1 and d_2 are the lengths of the solid section and the hole section, respectively (see the inset of Fig. 2). The effective index $n_{1\text{eff}}$ is defined by $n_{1\text{eff}} = n_z$, where n_z is the effective refractive index for the waveguide mode defined by $k_z = \omega n_z/c$, and k_z is the wavevector along the propagation direction. $n_{2\text{eff}}$ is defined by $n_{2\text{eff}} = (n_z * A_{\text{solid}} + n_{\text{hole}} * A_{\text{hole}})/(A_{\text{solid}} + A_{\text{hole}})$, where A_{solid} and A_{hole} are the areas occupied by the solid material and holes in the hole section, and n_{hole}

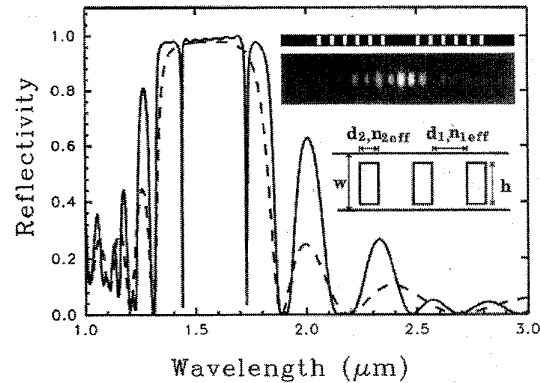


Fig. 2. Calculated reflection spectra of a 0.3 μm photonic wire mirror with six rectangular holes (dashed line) and the corresponding photonic wire microcavity (solid line). The insets show the geometry and field distribution in the microcavity. The cavity length is 0.775 μm , and six ($0.225 \times 0.1 \mu\text{m}^2$) holes are on either side to form a Fabry-Perot cavity.

is the refractive index in the holes. For our calculated example, A_{solid} and A_{hole} are 0.005 μm^2 and 0.025 μm^2 , respectively; n_{hole} is 1; and n_z is 2.869 for the fundamental mode in the waveguide. With the above formula, this gives $\lambda_B \approx 1.55 \mu\text{m}$.

In the limit where the hole width h is equal to the waveguide width W , the structure degenerates to the usual multilayer Bragg reflector. In this limit, $n_{1\text{eff}}/n_{2\text{eff}}$ has the largest value, and we expect the bandgap to be widest. Let us call this bandgap the maximum bandgap. For our calculated example, the gap shrinks to about 60% of this maximum bandgap. Hence, more holes are needed to reach high reflectivity compared with the limiting case.

Fig. 2 also graphs (solid line) the FD-TD calculated reflection spectrum for the photonic wire microcavity structure shown in Fig. 1 with a 0.79- μm -thick waveguide. In the calculation, the effect of the waveguide thickness is accounted for by computing the effective index of propagation in a 0.79 μm thick planar waveguide and using it as the bulk material index in the 2-D model. The reflectors are made up of six holes on either side of the wire with the same parameters as those used in simulating reflectors. The physical cavity length is chosen to be 0.875 μm , representing the distance between the centers of the two beginning holes on each side of the cavity. From the width of the resonance dip in Fig. 2, we estimate the cavity Q to be around 500. This value agrees approximately with the Q value obtained from the cavity field decay time observed computationally. By varying the structural parameters, we can adjust the number of resonant modes in the gap, the center frequency of the gap, and the gap bandwidth. We assume the operating wavelength to be 1.55 μm and the material to be an InGaAs-InGaAsP system. The calculated electric field of the resonant mode is also shown in the inset of Fig. 2.

Future numerical modeling aimed at improved accuracy will implement full-wave 3-D FD-TD simulations taking into account the finite height of the holes in the photonic wire. The major difference we expect will be the vertical diffraction effect in the hole region. As the electromagnetic field penetrates into the hole region, the small vertical extent

of the field defined by the waveguide height will likely lead to a substantial vertical diffraction, thereby contributing to loss. In order to minimize this effect, the ratio of waveguide height to hole length must be large.

III. FABRICATION PROCESS

As a step toward the realization of the proposed lasers, we have successfully fabricated suspended photonic wire structures with a multiquantum-well InGaAsP–InGaAs material system, which was grown by molecular beam epitaxy (MBE). Such suspended structures can be fabricated via a selective etching technique in a way analogous to the suspended bridge-like vertical mirror structure fabricated by Ho *et al.* with an AlGaAs–GaAs material system [9].

The waveguide structure was grown in the following manner. A 0.2- μm -thick InP buffer layer was first grown on the InP substrate, followed by the waveguide layer. The waveguide layer is comprised of eight 100- \AA quantum wells separated by 100- \AA barriers and sandwiched by two 0.32- μm -thick InGaAsP cladding. The total waveguide layer thickness is 0.79 μm .

Nanofabrication techniques were used in this process. First, an 800- \AA -thick SiO₂ layer was deposited on the InGaAsP–InGaAs wafer using plasma enhanced chemical vapor deposition (PECVD). PMMA was then spun on top of the SiO₂ to act as an electron-beam resist. The microcavity pattern was written in the PMMA with the JEOL JBX 5DII electron-beam (E-Beam) writer. After that, the pattern was transferred down to the SiO₂ layer using reactive ion etching (RIE), which was performed with CHF₃ as the etchant gas under 31 mtorr pressure and 60 W plasma power. The PMMA was then removed. The pattern on SiO₂ formed the mask for subsequent etching of the InGaAsP layer. RIE was again used to etch the photonic wire and holes down vertically through the 0.79- μm -thick epitaxial layer into the InP substrate. In this RIE step, we used a gas mixture of methane, hydrogen, and argon with a ratio of 10:34:10 under 45 mtorr pressure and 90 W plasma power. Finally, the suspended structures were formed using highly selective HCl etchant to remove the InP material beneath the epitaxial layer.

Fig. 3 shows scanning electron microscope (SEM) photos of the suspended photonic wire microcavities. Fig. 3(a) is a view before selective etching. Here, the bottom can be seen clearly. After selective etching, the material under the microcavity was removed, resulting in the structure shown in Fig. 3(b). The suspended microcavity is 11 μm in length, 0.45 μm in width, and 0.79 μm in thickness. In order to provide potentially high reflectivity, 20 holes were etched in the photonic wire. The success in the fabrication of the suspended structure is

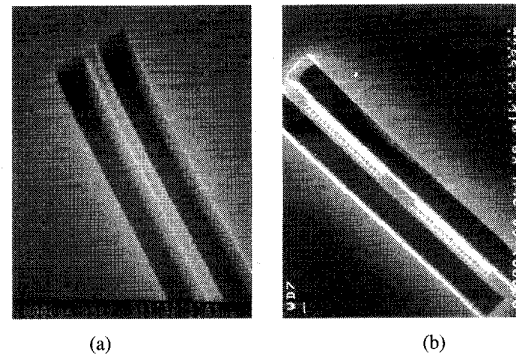


Fig. 3. (a) Scanning electron microscope (SEM) image of the microcavity before selective etching. (b) SEM image of a 0.45 μm suspended photonic wire microcavity.

an important step toward the realization of microcavity lasers based on photonic bandgap structures.

In summary, we have discussed a novel microcavity structure that combines a photonic bandgap reflector and a photonic wire. Our numerical simulations show that this type of reflector is broad-band (450 nm) and has high reflectivity (0.98) with only six rectangular holes. While the cavity Q can be as high as 500 for this case, vertical diffraction loss in the holes may place a limit on how thin the structure can be. We have successfully demonstrated the nanofabrication of a suspended structure of this type, which is an important step toward the realization of the corresponding microcavity lasers.

REFERENCES

- [1] S. L. McCall, A. F. J. Levi, R. E. Slusher, S. J. Pearton, and R. A. Logan, "Whispering-gallery mode microdisk lasers," *Appl. Phys. Lett.*, vol. 60, no. 3, pp. 289–291, 1992.
- [2] J. P. Zhang, D. Y. Chu, S. L. Wu, S. T. Ho, W. G. Bi, C. W. Tu, and R. C. Tiberio, "Photonic-wire lasers," *Phys. Rev. Lett.*, vol. 75, pp. 2678–2681, Oct. 1995.
- [3] D. Y. Chu and S. T. Ho, "Spontaneous emission from excitons in cylindrical dielectric waveguides and the spontaneous emission factor of microcavity ring lasers," *J. Opt. Soc. Amer. B*, vol. 10, pp. 381, 1993.
- [4] E. Yablonovitch, "Inhibited spontaneous emission in solid-state physics and electronics," *Phys. Rev. Lett.*, vol. 58, pp. 2059–2062, 1987.
- [5] D. Y. Chu and S. T. Ho, "Dielectric photonic well and wire and 1-D photonic bandgap structure in photonic wire," in *Optical Soc. Amer. Annu. Meet. Tech. Dig.*, San Jose, CA, Oct. 1991, paper MT5.
- [6] B. Meade and J. D. Joannopoulos, "Cavities in photonic bandgap material for laser applications," in *Optical Soc. Amer. Annu. Meet. Tech. Dig.*, San Jose, CA, Oct. 1991, paper MT1.
- [7] P. R. Villeneuve, S. Fan, J. D. Joannopoulos, K. Y. Lim, G. S. Petrich, L. A. Kolodziejski, and R. Reif, "Air-bridge microcavity," *Appl. Phys. Lett.*, vol. 67, no. 2, pp. 167–169, 1995.
- [8] A. Taflov, *Computational Electrodynamics: The Finite-Difference Time-Domain Method*. Boston, MA: Artech House, 1995.
- [9] S. T. Ho, S. L. McCall, R. E. Slusher, L. N. Pfeiffer, K. W. West, A. F. J. Levi, G. E. Blonder, and J. L. Jewell, "High index contrast mirror for optical microcavities," *Appl. Phys. Lett.*, vol. 57, no. 14, pp. 1387–1389, 1990.